Effect of Ship Propulsion Retrofit on Maneuverability Research Based on Co-simulation

Tongtong Wang[1(✉)], Lars Ivar Hatledal[2], Motoyasu Kanazawa[1], Guoyuan Li[1], and Houxiang Zhang[1]

[1] Department of Ocean Operations and Civil Engineering, Faculty of Engineering, Norwegian University of Science and Technology (NTNU), Aalesund, Norway
{tongtong.wang,motoyasu.kanazawa,guoyuan.li,hozh}@ntnu.no

[2] Department of ICT and Natural Sciences, Faculty of Information Technology and Electrical Engineering, Norwegian University of Science and Technology (NTNU), Aalesund, Norway
laht@ntnu.no

Abstract. Shipping has been dominating the transportation industry in worldwide trade. During the service life of a vessel, conversions in mid-life often occur for economic or technical purposes. By replacing expired components or updating the outdated technology to the latest operational standards, the service life could be greatly prolonged, and meanwhile the capability will be enhanced. Bringing ships-in-service to the latest technology creates the need for advanced methods and tools to simulate the ship main and auxiliary systems. Co-simulation is emerging as a promising technique in complex marine system modeling. The Functional Mock-up Interface (FMI) standard enables sub-models representing part of the vessel to be executed individually or as an integrated part of the overall system. The modularity and re-usability of the sub-models speed up the simulation cycle and ensure time-cost effectiveness, which benefits the ship conversion. This paper presents a research related to the ship propulsion retrofit process based on the co-simulation technique. The ship maneuverability before and after refitting propulsion units is simulated and analyzed. Through the experiments, propulsion performance improvements are observed. Eventually, the study supports that the co-simulation technique to be applied in the maritime field has an encouraging future.

Keywords: Propulsion retrofit · Ship maneuverability · Co-simulation

1 Introduction

Shipping, as a relatively energy-efficient, environmental-friendly, and sustainable model of mass transport, is the dominant transportation method for world-wide

This work was supported by a grant from the Research Council of Norway through the Knowledge-Building Project for industry "Digital Twins for Vessel Life Cycle Service" (Project no: 270803).

A. Cerone et al. (Eds.): SEFM 2021 Workshops, LNCS 13230, pp. 189–203, 2022.
https://doi.org/10.1007/978-3-031-12429-7_14

trade. Normally, the life cycle of a ship is estimated to be around 25 years, but the actual age of the short sea fleet, for example, is higher, reaching more than 30–35 years of age for perhaps as much as 40% of the fleet [9]. However, the life cycle of ship systems and major components is much shorter because of the ever faster technological developments. In general, 10–15 years after launching a ship, its main systems are outdated. Upgrading outdated technology in ships to the latest operational standards enhances the capability and prolongs the service life [13]. Furthermore, the international policies fostering the reduction of energy consumption and emissions are always issuing new regulations on energy efficiency and emission reduction [3]. For example, the International Maritime Organization (IMO) has implemented a stricter sulfur content limit–called the IMO 2020 sulfur cap–aiming at improve air quality and protect the environment. Further, IMO has initiated an extensive strategy of the energy efficiency existing ship index for existing ships, which indicate that the energy efficiency of ships should be satisfied during the operation phase. To comply with the new regulations, green technologies are implemented on-board ships [10]. Retrofitting the ships during the operation phase has become a popular choice for the transportation industry [15]. It is possible to upgrade the installed technology with new high-performance machines and significantly improve the system's handling, economic efficiency, as well as emission reduction [8].

Given that modern ships are becoming more complex and integrated, retrofitting them is a complex and intricate engineering task. Optimal performance is relying on all subsystems to work optimally, both individually and aggregated [11,14]. Each subsystem is dedicated to a specific object of the vessel or equipment. Between distributed components, they exchange all relevant ship information, data, or analysis and make coordinated operational decisions. Considering the mutual and multi-disciplinary interaction between subsystems, co-simulation is emerging as a promising technique. Often, it is difficult to describe a truly complex system in a single tool. Instead, people are encouraged to develop models at the partial solution level, such as the dynamic properties check, control strategy design, or energy consumption optimization. It not only dramatically lessens the modeling pressure and promotes efficiency but enables the re-usability of different elements. Furthermore, a branch of components may be generated by different teams or suppliers, each in its own domain and each with its own tools. Using co-simulation, these models can be integrated as black-boxes without revealing the intellectual property of the owner [2]. In addition, considering now the demanding operation of an autonomous vessel, it is better to test ahead in a virtual environment for safety reasons. Co-simulation reduces efforts to conduct pre-training or perform tests by redirecting design attention and reusing the sub-system models. From an efficiency point of view, co-simulation greatly facilitates the ship retrofitting process.

In a co-simulation, different subsystems are modeled separately and composed into a global simulation, where each model is executed independently, sharing information at discrete time points. The Functional Mock-up Interface (FMI) standard is a commonly used standard for co-simulation, and model imple-

Fig. 1. Side view of the research vessel Gunnerus.

menting the FMI is known as a Functional Mock-up Unit (FMU). The FMI enables an FMU exported by one tool to interoperate with a variety of host tools and for host tools to orchestrate interactions between FMUs exported by a variety of other tools [1]. A system can then be modelled as a collection of interconnected FMUs. Co-simulation thus enables retrofit decisions to be simulated ahead-of-time, cheaply and early in the process.

This study presents the propulsion retrofit process using the co-simulation technique, and the dynamic properties of the retrofitted devices are analyzed and discussed. The research vessel Gunnerus (see Fig. 1), owned and operated by the Norwegian University of Science and Technology (NTNU) serves as the test ship. The simulation fidelity was verified against real ship maneuver in [7] in terms of ship speed, course, and power consumption. Convinced by the high-fidelity resolution of the simulation, further research is conducted with more confidence. As reported in [16], The R/V Gunnrus went through a thruster refit in 2015. The original twin fixed-pitch ducted propellers and rudders were replaced with the Permanent Magnet (PM) rim-drive azimuthing thrusters. The original propellers were 5-bladed, high skew type with a diameter of 2.0 m that rotated in a 19 A type duct profile, and the new azimuthing thrusters incorporates a ring propeller in a tailor-made duct with a diameter of 1.9 m with four blades having a forward skewed shape. Figure 2 shows the propulsion configuration on Gunnerus before and after retrofit, where the left is the origin pitch propeller with ice-fins, and the right is the refitted azimuth thruster provided by Rolls-Royce. The same diesel-electric system supplied the propulsion and maneuvering power before and after the conversion. To document the effect of the change of propulsion system, a simulation test is carried out both before and after retrofitting the

Fig. 2. The propulsion arrangement before and after retrofit.

PM azimuthing thruster in this work. The ship maneuvering capabilities are then verified.

2 Problem Formulation

Thanks to the modularity and flexibility of co-simulation, the effort required to simulate the dynamic properties of the propulsion unit is greatly decreased. In this section, the ship maneuverability and the co-simulation diagram, as well as the FMUs used in this research will be explained.

2.1 Ship Maneuverability

Ship maneuverability is defined as the capability of the craft to carry out specific maneuvers. A maneuvering characteristic can be obtained by changing or keeping a predefined course and speed of the ship in a systematic manner by means of active controls. For most of the surface vessels, these controls are implemented by rudders, propellers and thrusters. The IMO approved standards for ship maneuverability, and the standards specify the type of standard maneuvers and associated criteria. It is always necessary for the vessels to apply these standards, and even some port and flag states adopted some of the IMO standards as their national requirements. To help the vessel prepare for implementation of the standards, prediction of the maneuverability performance in the design stage enables a designer to take appropriate measures in good time to achieve requirements. The prediction could be carried out by using existing data, scaled model test, or numerical simulation [12]. From the practical view, numerical simulation appears an effort-efficient way. Therefore, the ship maneuvering capabilities will be the main concern during simulation experiments.

To examine the course keeping capability of the ship, usually, the turning circle and Kempf's zigzag maneuver are selected. The maneuvers and their characteristic are described as Fig. 3 and Table 1 and 2:

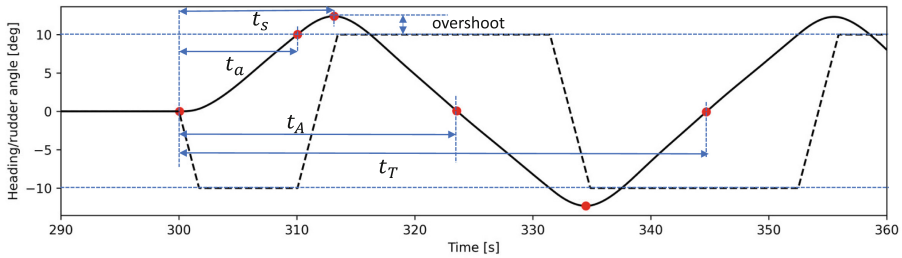

Fig. 3. Schematic of zigzag maneuver and its main characteristics.

Table 1. Zigzag maneuver characteristics.

Characteristic	Reference
Initial turning time t_a	The time from the rudder execution until the heading changes a desired degrees, 10° off the initial course in 10°/10° example
Time to check yaw t_s	The time from the rudder execution until the maximum heading changes
Reach time t_A	The time between the first rudder execution and the instance when the ship's heading is zero
Complete time t_T	The time between the first rudder execution and the instance when the ship's heading is zero after third execution
Overshoot angle	The angle through which the ship continues to turn in the original direction after execution of counter rudder

2.2 Co-simulation Setup

The ship maneuvering simulation is set up as Fig. 4 shows. Each block represents an FMU of which the input and output variables are declared. The experiment is performed in Vico, a generic co-simulation framework based on the Entity-Component-System software architecture that supports the FMI as well as the System Structure and Parameterization (SSP) standards [5]. The user may manipulate the wind, waves, and ocean currents to mimic environmental conditions. An overview of FMUs applied in the maneuvering simulation is presented. All the FMUs, except the *VesselModel* and *PMAzimuth*, are developed by the authors using PythonFMU [6].

1. **VesselModel**
   The vessel model reflects the vessel's hydrodynamic properties, such as the

Table 2. Turning circle maneuver and its main characteristics.

Characteristic	Unit
Steady turning radius	m
Transfer at 90° heading	m
Advance at 90° heading	m
Maximum transfer	m
Maximum advance	m
Tactical diameter at 180° heading	m

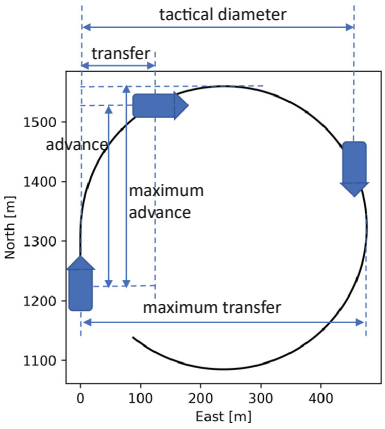

mass, resistance, and cross-flow drag, as well as restoring forces. It is a 6° of freedom (DOF) time-domain simulation model developed by MARINTEK's vessel simulator (VeSim) [4]. Summing all the external forces acting on the ship, the dynamic equations of vessel motions are then solved. It can be implemented in sea-keeping and maneuvering problems for marine vessels subjected to waves, wind, and currents based on a unified nonlinear model Eq. 1.

$$(M_{RB} + M_A)\dot{\nu} + C(\nu)\nu + D(\nu) + g(\eta) + \int_0^t h(t-\tau)\nu(\tau)\,d\tau = q \qquad (1)$$

where the 6DOF ship velocity state is expressed as the vector $\nu = [u, v, w, p, q, r]'$ referred to the coordinate shown in Fig. 5. The $[u, v, w]$ are the linear velocity along x_b, y_b, z_b directions, and $[p, q, r]$ are the angular velocities rotating around three directions. $M_{RB} \in \mathbb{R}^{6\times6}$ is the rigid body mass, and $M_A \in \mathbb{R}^{6\times6}$ is the added mass. $C(\nu) = C_{RB}(\nu) + C_A(\nu) \in \mathbb{R}^{6\times6} \times \mathbb{R}^6$ is describing the generalized coriolis-centripetal forces. $D(\nu) \in \mathbb{R}^{6\times6} \times \mathbb{R}^6$ is a vector of damping forces and moments. $g(\eta) \in \mathbb{R}^6$ is a vector of gravitational/buoyancy forces and moments. And $h(\tau)$ refers to impulse response functions calculated by SINTEF OCEAN's potential theory. $q \in \mathbb{R}^6$ is the external forces and moments acting on the ship. The model itself is fully coupled and it can be used for simulation and prediction of coupled vehicle motion.

2. **PID controller**
The PID controller is created to generate shaft speed and rudder angle commands according to Eq. 2. In the control law, the $k_{\{.\}}$ is the parameter enabling tuning, and the predefined approach speed u_d as well as the ship

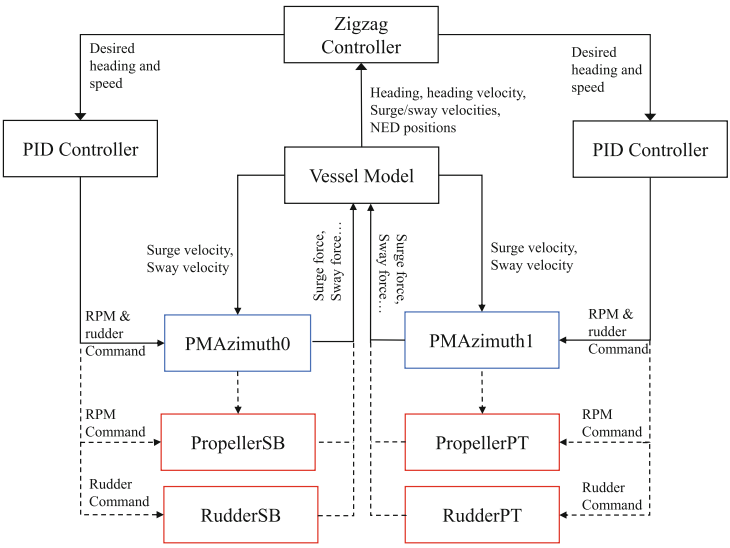

Fig. 4. Diagram showing the relationship of the engaged ship components.

heading ψ_d are issued by the *ZigzagController*.

$$\begin{aligned} RPM &= k_{pu}(u - u_d) + k_{iu}\int_0^t (u - u_d)dt + k_{du}\frac{d}{dt}(u - u_d) \\ \delta &= k_{ppsi}(\psi - \psi_d) + k_{ipsi}\int_0^t (\psi - \psi_d)dt + k_{dpsi}\frac{d}{dt}(\psi - \psi_d) \end{aligned} \tag{2}$$

3. **Zigzag controller**
   It is a logistic solver without numerical computation. Given the current ship speed and heading, it can tell to which side the rudder should turn and deliver the command saturation to the connected *PID controller*.
4. **PMAzimuth**
   It is a hydrodynamic model of the azimuth thruster without actuator, implemented by the manufacturer Kongsberg Maritime using VeSim. Feeding a specific RPM and angle command, vessel speed, as well as the loss factor into the model, it produces a 3DOF force on heave, surge, and sway directions.
5. **Propeller**
   Both the propeller and rudder are generic models parametrized to R/V Gunnerus. The surge force related to the propeller is calculated with:

$$\tau_p = f(n, u) \tag{3}$$

where n is the propeller shaft speed (r/min), and u is the vessel's surge velocity. Note that the sway force and yaw moment due to propeller are neglected as they have smaller magnitudes compared to those of hull and rudder components.

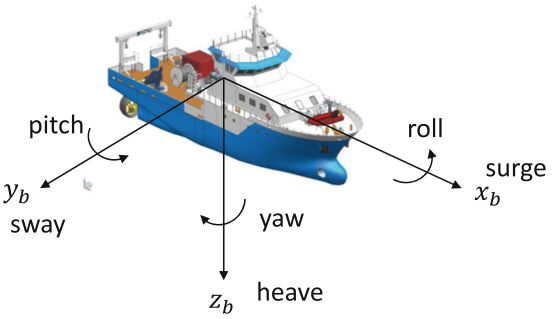

Fig. 5. The ship body coordinate and motion in 6DOF.

6. **Rudder**
   The rudder is modelled according to [17]. It can be expressed as:

$$\tau_r = g(u, v, r, n, \delta, \theta) \tag{4}$$

   where u, v, r are the velocities in surge, sway, and yaw directions respectively. And δ is the rudder angle. θ refers to the hull-rudder interaction coefficients.

3 Experiment Results

Experiments are implemented with the designed co-simulation diagram in Vico. The detailed experimental scenarios and the corresponding ship maneuverability, with either pitch propeller or PMAzimuth thruster installed, are presented in this section.

3.1 Simulation Scenarios

Ship maneuvering experiments with a different set of propulsion units are implemented. It is also worth noticing that the ship maneuverability could be affected by water depth, environmental forces, ship speed and hydrodynamic derivatives. To ensure the results comparable, identical settings except only the propulsion units are employed. The ship is assuming cruising on calm and deep water without external environmental disturbances. Eight maneuver test scenarios are defined as Table 3 shows, aiming to investigate the propulsion performance under different execution angles and speeds.

A $10° - 10°$ zigzag test means that the rudder and azimuth angles are given a command of $\pm 10°$, and when the ship heading change reaches $10°$ the rudder/azimuth reverse to the opposite side. The $10°$ in turning circle refers to the constant rudder/azimuth angle. As a key parameter, the ship surge speed is given as the steady velocity before the zig-zag/turning circle maneuvers are initiated. During the process, 300 s are saved first to warm up and drive the ship to the pre-defined speed, and 300 s are arranged for operations. The simulation time step is set to 0.05 s.

3.2 Results Analysis

In this section, the main maneuver characteristics of the ship before and after conversion will be observed and discussed.

Zigzag Maneuver. Zigzag trajectories for the ship using both the pitch propellers and azimuth thrusters are simulated. Three selected test results are presented and compared in Fig. 6, 7 and 8. Naturally, differences in turning velocities are observed from these figures. A more noticeable yaw velocity distinction between the pitch propeller and azimuth arises during 10° turn command. The

Table 3. Maneuver experiment cases implemented in Vico.

Maneuver	Execution	Speed
Zig-zag	10° − 10°	low
		High
	20° − 20°	Low
		High
Turning circle	10°	Low
		High
	20°	Low
		High

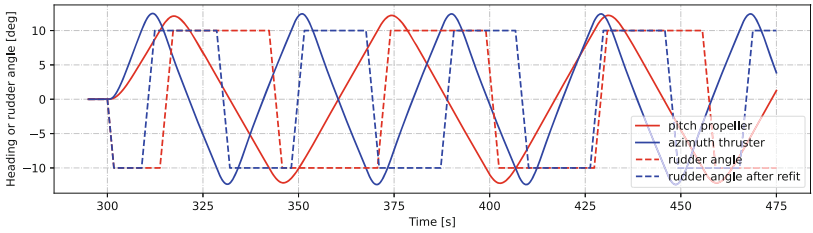

(a) 10°/10° zigzag ship heading and command angle at higher speed.

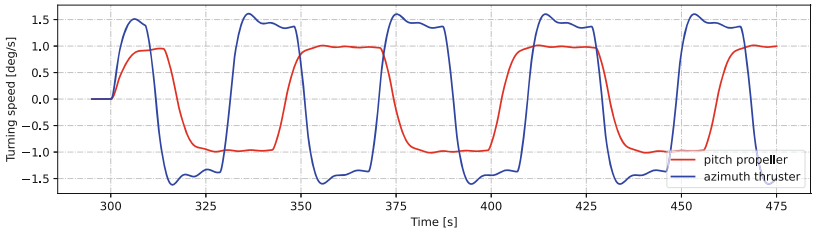

(b) Ship turning velocities under propeller or azimuth actuation.

Fig. 6. 10°/10° zigzag properties at higher speed.

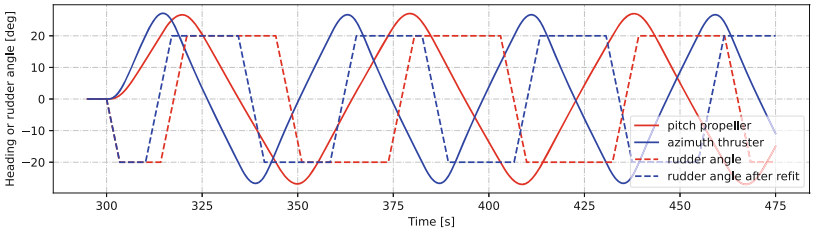

(a) 20°/20° zigzag ship heading and command angle at higher speed.

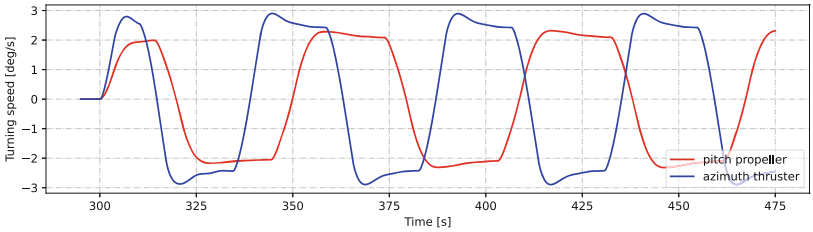

(b) Ship turning velocities under propeller or azimuth actuation.

Fig. 7. 20°/20° zigzag properties at higher speed.

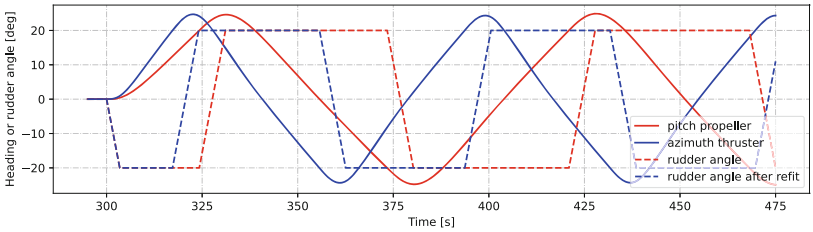

(a) 20°/20° zigzag ship heading and command angle at lower speed.

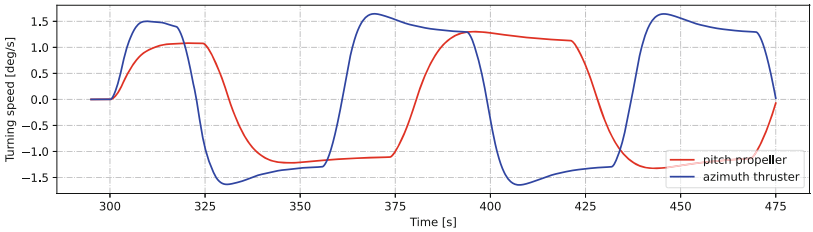

(b) Ship turning velocities under propeller or azimuth actuation.

Fig. 8. 20°/20° zigzag properties at lower speed.

Table 4. The zigzag characteristics for the ship before and after propulsion unit retrofit.

Characteristics		10°/10°			10°/10°			20°/20°			20°/20°		
		pr	azi	gain [%]	pr	azi	gain [%]	pr	azi	gain [%]	pr	azi	gain [%]
Approach speed	[m/s]	4.7	4.78	–	2.4	2.5	–	4.7	4.73	–	2.45	2.47	–
t_a	[s]	13.7	8.9	35	24.25	15.6	35.7	8.95	6.45	27.9	14.9	10.4	30.2
t_s	[s]	3.6	2.9	19.4	5	3.6	28	10.8	8.25	23.6	16.3	12.2	25.2
t_A	[s]	31.9	21.3	33.2	54.4	35.25	35.2	34.5	26.25	23.9	55.6	40.7	26.8
t_T	[s]	60.3	40.75	32.4	103.2	67	35.1	64.15	50.3	21.6	103.8	78.75	24.1
First overshoot angle	[°]	2.17	2.37	−9.2	1.57	1.6	−1.9	6.64	6.7	−0.9	4.6	4.7	−2.1
Second overshoot angle	[°]	2.2	2.42	−10	1.58	1.61	−1.9	6.87	6.68	2.8	4.8	4.36	9.2
Average overshoot angle	[°]	2.2	2.42	−10	1.576	1.6	−1.5	7.01	6.7	4.4	4.92	4.35	11.6

statistic results are summerized in Table 4. It could be observed that the measured key time parameters in the azimuth group are effectively decreased. This conclusion reveals that the ship with azimuth installed reaches the desired course within a shorter time, and it responds more quickly to the given command.

Meanwhile, it is observed in Fig. 6 that the rudder rate of both systems are similar, as they reverse from port-side to starboard in a similar amount of time. Although it takes longer time for the ship using conventional rudders to drive itself to the target course, it does not necessarily generate a larger overshoot angle. Instead, their average overshoot angles are related to the execution command and maneuver speed as indicated in Table 4. If a smaller angle command is given to the azimuth, it would even lead to a slightly larger average overshoot angle compared to the conventional rudder, even with a lower or higher forward speed. With an increasing angle command, the azimuth thrusters are observed to perform outstandingly.

Turning Circle. The turning circle maneuver experiments are conducted under the resembling co-simulation structure (Fig. 4) but replacing the *Zigzag controller* with *Turning controller*. The execution angle and speed are distinguished into two categories: 10° and 20°, higher and lower approach speed, respectively.

The statistical maneuver results are presented in Table 5. Among the four cases, two of them are selected to visualize the differences (See Fig. 9 and 10).

Table 5. The turning characteristics for the ship before and after propulsion unit retrofit.

Characteristics		10°			10°			20°			20°		
		pr	azi	gain [%]	pr	azi	gain [%]	pr	azi	gain [%]	pr	azi	gain [%]
Approach speed	[m/s]	4.7	4.8	–	2.4	2.5	–	4.7	4.7	–	2.4	2.5	–
Steady turning radius	[m]	237.5	185.5	21.9	237.8	186.3	21.6	90.4	91.3	−1	93.2	92.9	0.32
Maximum transfer	[m]	476.2	370.6	22.2	476.4	371.9	21.9	190.7	184.8	3.1	195.1	187.7	3.8
Maximum advance	[m]	266.7	200.5	24.8	265.5	200.3	24.5	127.8	108.9	14.8	128.3	109.6	14.6
Transfer	[m]	227.5	173.7	23.6	227.2	173.9	23.4	88.1	82.2	6.7	88.8	82.5	7.1
Advance	[m]	266.4	200.1	24.9	265.2	199.9	24.6	127	108.1	14.9	127.4	108.7	14.7
Tactical diameter	[m]	475.9	370.2	22.2	476.1	371.5	22.0	189.96	184.1	3.1	194.2	186.9	3.8

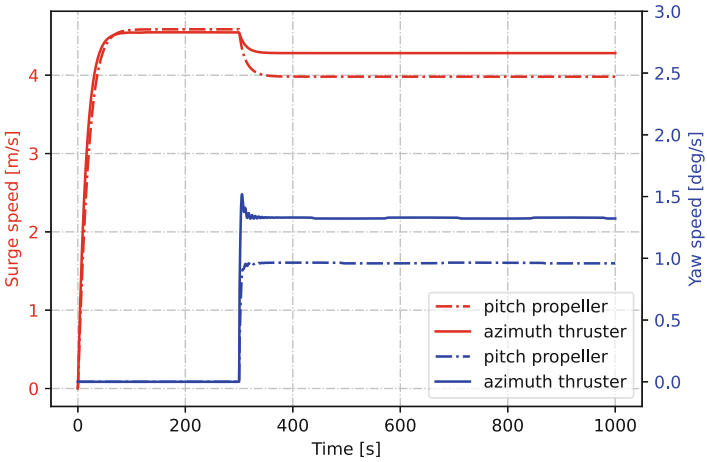

(a) The ship's surge and yaw speed when circling at 10° with a fast speed.

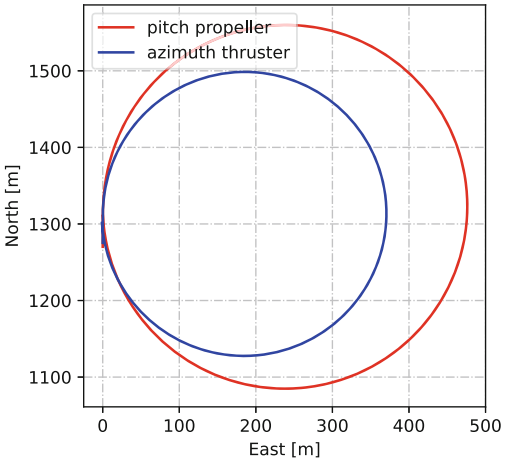

(b) Comparison of propeller and azimuth actuated ship trajectories.

Fig. 9. 10° turning circle properties at higher speed.

The ship equipped with either the conventional pitch propellers and rudders, or azimuths, are approaching at similar speeds before execution. From Fig. 9a, a drop of surge speed is observed when the rudder is instantiated, and the drop of pitch propeller is more obvious compared to that of the azimuth. Meanwhile, a larger turning velocity is offered by the azimuth. The out-performance in response velocities is expected to lead to a narrowed turning radius which is verified in Fig. 9b.

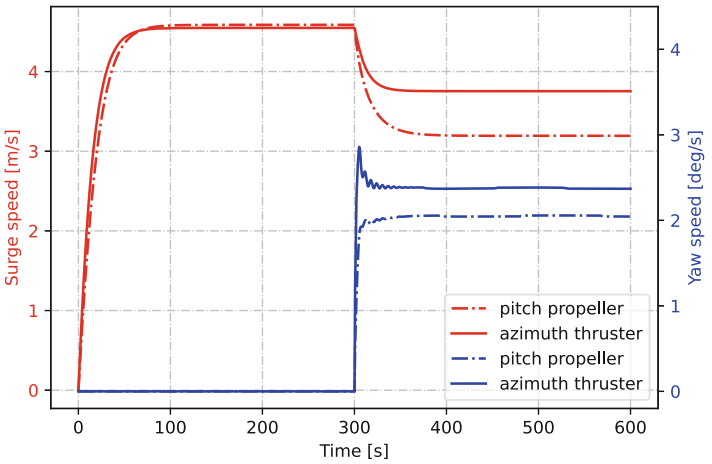

(a) The ship's surge and yaw speed when circling at 20° with a fast speed.

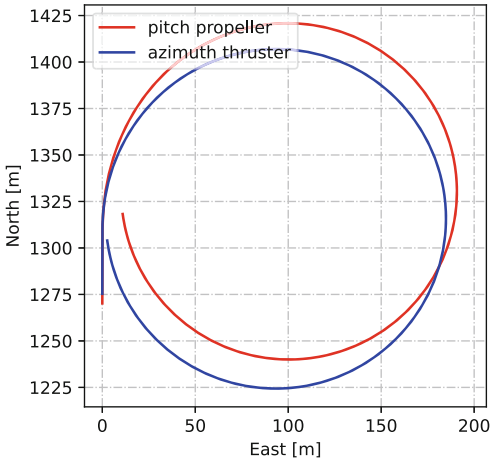

(b) Comparison of propeller and azimuth actuated ship trajectories.

Fig. 10. 20° turning circle properties at higher speed.

Moreover, the statistical results show that the angle command affects the propulsion performance more than the approach speed. Comparing Fig. 9 and Fig. 10, the ship exhibits similar speeds before operation. However, the percentage of decreased surge velocity with 20° rudder angle is higher than that with 10° counter angle. For the azimuth thruster, it drops about 6% in 10° and 19% in 20°. For the propeller, the values are 15% and 32%. When the rudder angle is given 20°, it not necessarily generates a large turning radius, as the propulsion moments could produce a higher yaw rate compared to 10°. This finding leads

to a compromise in overall turning performance. Therefore, it is understandable that the steady radius reduction at 20° command is smaller than that of the lower command.

4 Conclusion

The continuously improving knowledge and availability of high-performance machines and drives have created the need for advanced methods and tools to facilitate retrofitting existing ships. Usually, the retrofit is driven by environmental and/or technical reasons, such as to comply with new energy regulations or to upgrade outdated technology. Either way, it is beneficial to ensure fast refitting procedures by allowing easier integration of new components. Co-simulation reduces both the time and the costs of refitting procedures, extending the operative life of a vessel in service. In this research, the authors utilized the co-simulation techniques to model the ship maneuver process before and after propulsion conversion and evaluate the impact of new devices on the ship maneuverability, aiming to support decisions on measures to meet operational standards. By comparing the zigzag and turning circle maneuver characteristics in the present work, an improved course keeping capability is observed after refitting advanced permanent magnet driven azimuth thrusters on the ship. This practice supports that co-simulation enables time cost-effective redesign and fast virtual tests by taking advantage of its modularity and flexibility, and emerges as a promising technology in the maritime industry.

However, it should be clarified that the quality of the simulation model may vary, and the tests conducted in order to compare the maneuvering performance of the two systems, and are not necessarily a good measure of the daily maneuvering capabilities of the vessel. Agreeing with this situation, the experiments performed through co-simulation will be qualitatively informative so that the comparative conclusions drawn upon are credible.

In the present study, only the ship maneuvering performance investigation is within scope, but in many cases, energy consumption is the major concern. Therefore, further research on the energy cost of the ship with different propulsion sets installed will be implemented by taking advantage of co-simulation technology in the future.

References

1. Broman, et al.: Determinate composition of FMUS for co-simulation. In: 2013 Proceedings of the International Conference on Embedded Software (EMSOFT), pp. 1–12. IEEE (2013). https://doi.org/10.1109/EMSOFT.2013.6658580
2. Gomes, C., Thule, C., Broman, D., Larsen, P.G., Vangheluwe, H.: Co-simulation: a survey. ACM Comput. Sur. (CSUR) **51**(3), 1–33 (2018). https://doi.org/10.1145/3179993
3. Halff, A., Younes, L., Boersma, T.: The likely implications of the new IMO standards on the shipping industry. Energy Policy **126**, 277–286 (2019). https://doi.org/10.1016/j.enpol.2018.11.033

4. Hassani, V., Ross, A., Selvik, Ø., Fathi, D., Sprenger, F., Berg, T.E.: Time domain simulation model for research vessel gunnerus. In: International Conference on Offshore Mechanics and Arctic Engineering, vol. 56550, p. V007T06A013. American Society of Mechanical Engineers (2015). https://doi.org/10.1115/OMAE2015-41786
5. Hatledal, L.I., Chu, Y., Styve, A., Zhang, H.: Vico: an entity-component-system based co-simulation framework. Simul. Model. Pract. Theory **108**, 102243 (2021). https://doi.org/10.1016/j.simpat.2020.102243
6. Hatledal, L.I., Collonval, F., Zhang, H.: Enabling python driven co-simulation models with PythonFMU. In: Proceedings of the 34th International ECMS-Conference on Modelling and Simulation-ECMS 2020. ECMS European Council for Modelling and Simulation (2020). https://doi.org/10.7148/2020-0235
7. Hatledal, L.I., Skulstad, R., Li, G., Styve, A., Zhang, H.: Co-simulation as a fundamental technology for twin ships (2020). https://doi.org/10.4173/mic.2020.4.2
8. Hou, H., Krajewski, M., Ilter, Y.K., Day, S., Atlar, M., Shi, W.: An experimental investigation of the impact of retrofitting an underwater stern foil on the resistance and motion. Ocean Eng. **205**, 107290 (2020). https://doi.org/10.1016/j.oceaneng.2020.107290
9. Koenig, P., Nalchajian, D., Hootman, J.: Ship service life and naval force structure. Nav. Eng. J. **121**(1), 69–77 (2009). https://doi.org/10.1111/j.1559-3584.2009.01141.x
10. Li, K., Wu, M., Gu, X., Yuen, K., Xiao, Y.: Determinants of ship operators' options for compliance with IMO 2020. Transp. Res. Part D: Transp. Environ. **86**, 102459 (2020). https://doi.org/10.1016/j.trd.2020.102459
11. Ling-Chin, J., Roskilly, A.: Investigating a conventional and retrofit power plant on-board a roll-on/roll-off cargo ship from a sustainability perspective-a life cycle assessment case study. Energy Convers. Manage. **117**, 305–318 (2016). https://doi.org/10.1016/j.enconman.2016.03.032
12. Liu, J., Hekkenberg, R., Rotteveel, E., Hopman, H.: Literature review on evaluation and prediction methods of inland vessel manoeuvrability. Ocean Eng. **106**, 458–471 (2015). https://doi.org/10.1016/j.oceaneng.2015.07.021
13. Liu, L., Yang, D.Y., Frangopol, D.M.: Ship service life extension considering ship condition and remaining design life. Mar. Struct. **78**, 102940 (2021). https://doi.org/10.1016/j.marstruc.2021.102940
14. Mauro, F., La Monaca, U., la Monaca, S., Marinò, A., Bucci, V.: Hybrid-electric propulsion for the retrofit of a slow-tourism passenger ship. In: 2020 International Symposium on Power Electronics, Electrical Drives, Automation and Motion (SPEEDAM), pp. 419–424. IEEE (2020). https://doi.org/10.1109/SPEEDAM48782.2020.9161920
15. Peri, D.: Robust design optimization for the refit of a cargo ship using real seagoing data. Ocean Eng. **123**, 103–115 (2016). https://doi.org/10.1016/j.oceaneng.2016.06.029
16. Steen, S., Selvik, Ø., Hassani, V.: Experience with rim-driven azimuthing thrusters on the research ship Gunnerus. In: Proceedings of High-Performance Marine Vessels (2016)
17. Yasukawa, H., Sakuno, R.: Application of the MMG method for the prediction of steady sailing condition and course stability of a ship under external disturbances. J. Mar. Sci. Technol. **25**(1), 196–220 (2019). https://doi.org/10.1007/s00773-019-00641-4